NANO LETTERS

pubs.acs.org/NanoLett

Letter

High-Speed Super-Resolution Imaging Using Protein-Assisted DNA-PAINT

Mike Filius, Tao Ju Cui, Adithya N. Ananth, Margreet W. Docter, Jorrit W. Hegge, John van der Oost, and Chirlmin Joo*

Cite This: *Nano Lett.* 2020, 20, 2264–2270

Read Online

ACCESS | Metrics & More | Article Recommendations | Supporting Information

ABSTRACT: Super-resolution imaging allows for the visualization of cellular structures on a nanoscale level. DNA-PAINT (DNA point accumulation in nanoscale topology) is a super-resolution method that depends on the binding and unbinding of DNA imager strands. The current DNA-PAINT technique suffers from slow acquisition due to the low binding rate of the imager strands. Here we report on a method where imager strands are loaded into a protein, Argonaute (Ago), which allows for faster binding. Ago preorders the DNA imager strand into a helical conformation, allowing for 10 times faster target binding. Using a 2D DNA origami structure, we demonstrate that Ago-assisted DNA-PAINT (Ago-PAINT) can speed up the current DNA-PAINT technique by an order of magnitude, while maintaining the high spatial resolution. We envision this tool to be useful for super-resolution imaging and other techniques that rely on nucleic acid interactions.

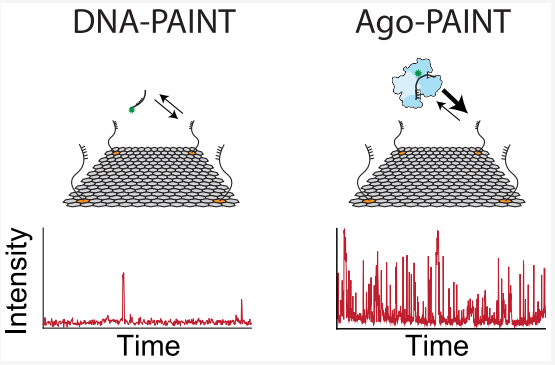

KEYWORDS: *DNA-PAINT, super-resolution microscopy, Ago-PAINT, single-molecule FRET, Argonaute, DNA origami*

Single-molecule localization microscopy techniques allow researchers to image cellular structures that are not visible through diffraction-limited microscopy methods. Most single-molecule localization techniques rely on the stochastic blinking of a fluorescent signal, by using photoswitchable fluorophores as in photoactivated localization microscopy (PALM)[1] and (direct) stochastic optical reconstruction microscopy ((d)-STORM).[2] An alternative approach to achieve stochastic blinking is through fluorescent probes that transiently bind their target, as in point accumulation in nanoscale topography (PAINT).[3−5]

In DNA-PAINT, a fluorophore is attached to a short DNA oligonucleotide, called an imager strand, that specifically binds to a complementary target DNA sequence, called a docking strand.[6] The stochastic blinking of signals is achieved through binding and unbinding of the incoming imager strands to the docking strands and is imaged using total internal reflection fluorescence (TIRF). By changing the length and sequence of an imager strand, one can tune the on- and off-rates of the imager and adjust the specificity. This allows for high multiplexing capabilities since the number of probes is only limited by the number of orthogonal DNA sequences. Furthermore, compared to conventional super-resolution techniques, DNA-PAINT comes with the advantage that imager strands are continuously replenished from the solution, and thus photobleaching is circumvented during the imaging process.

A critical limitation of DNA-PAINT, however, is the low binding rate of DNA, which is typically in the order of 10^6 M^{-1} s^{-1}. Given this binding rate, obtaining images with a high spatial resolution (5 nm) usually takes several hours.[7−9] Shorter acquisition times can be achieved by increasing the concentration of the imager strand. However, single-molecule binding events become unresolvable from the background of unbound imager strands, even when TIRF is used. To reduce this acquisition time, DNA-PAINT was recently combined with a single-molecule Förster resonance energy transfer (smFRET).[10,11] This, however, comes at a cost of reduced spatial resolution due to reduced energy transfer efficiency and due to limited choice of dyes. Here we describe an alternative approach, in which protein-assisted delivery of imager strands is demonstrated to speed up the acquisition time 10-fold and only to require a single fluorescence channel.

Argonaute proteins (Agos) are a class of enzymes that utilize a DNA or RNA guide to find a complementary target, either to inactivate or to cleave it. In eukaryotes, an RNA guide directs Ago to complementary RNA targets for post-transcriptional

Received: October 16, 2019
Revised: March 4, 2020
Published: March 13, 2020

https://dx.doi.org/10.1021/acs.nanolett.9b04277
Nano Lett. 2020, 20, 2264–2270

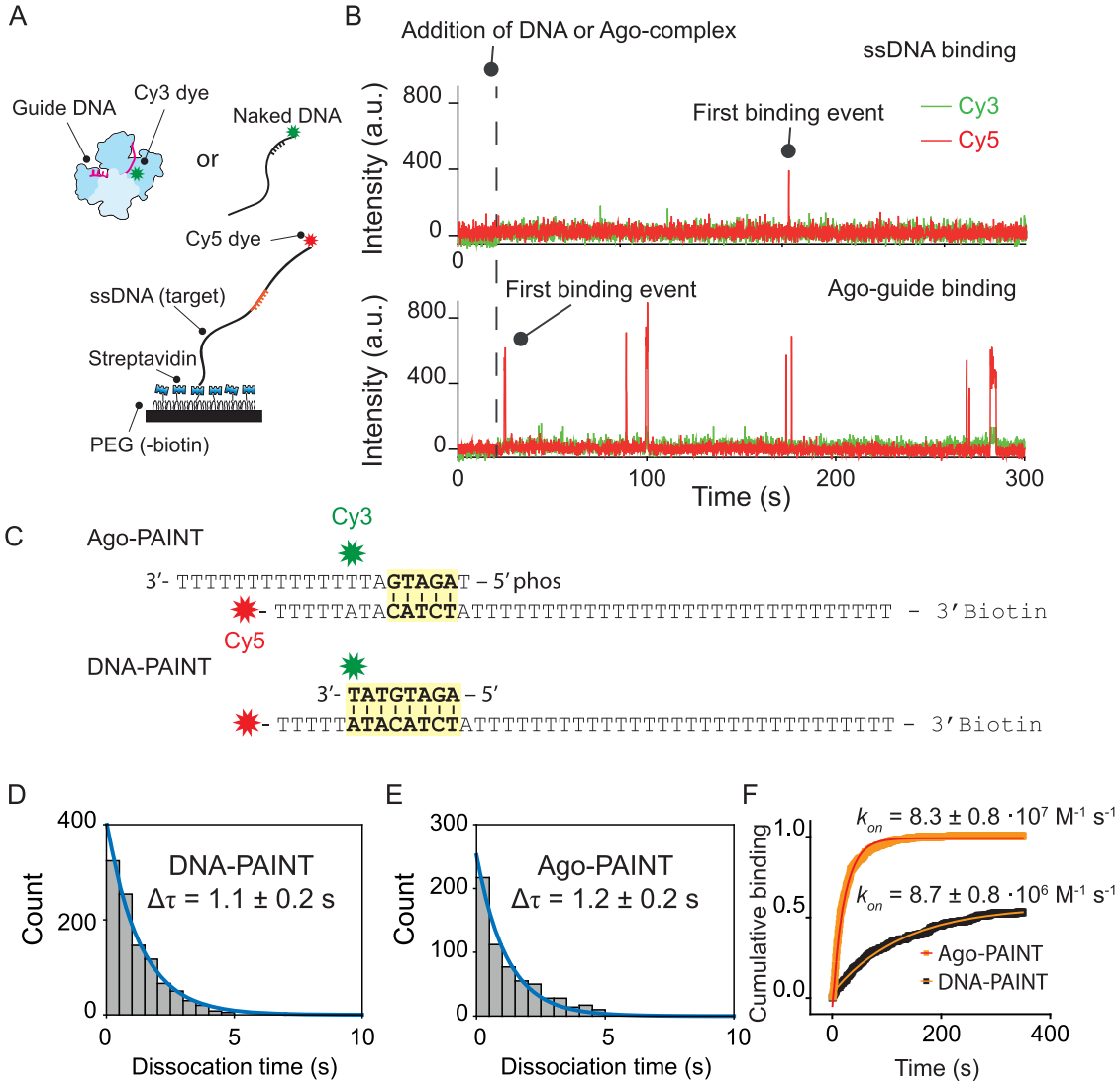

Figure 1. Single-molecule FRET assay to quantify binding kinetics Ago-PAINT vs DNA-PAINT. (A) A schematic of the single-molecule FRET assay with the target strand immobilized on a PEGylated surface through biotin−streptavidin conjugation. The green and red stars indicate the Cy3 and Cy5 dye, respectively. Binding of the Ago-guide complex or ssDNA probe to the ssDNA target results in a high FRET signal. (B) Representative traces of ssDNA binding (top) and Ago-complex binding (bottom). The dashed line indicates the time point at which the Ago-guide or DNA is iintroduced inside the microfluidic chamber. (C) A schematic of the sequences used for Ago-PAINT and DNA-PAINT. Upon binding, both constructs will give rise to a high FRET signal. (D) Dwell-time histogram ($\Delta\tau$) of ssDNA (sequence shown in Figure 1C). Maximum likelihood estimation (MLE) gives 1.1 ± 0.2 s as the parameter for a single-exponential distribution (blue line). Number of data points: 1029. (E) Dwell-time histogram ($\Delta\tau$) of Ago (sequence shown in Figure 1C). MLE gives 1.2 ± 0.2 s as the parameter for a single-exponential distribution (blue line). Number of data points: 696. (F) Cumulative binding event plots of DNA-PAINT (black) and Ago-PAINT (orange) vs time. A single exponential fit is used for DNA-PAINT (red line) and Ago-PAINT (orange line). Errors in panels D−F are determined by taking the 95% interval of 105 bootstraps.

regulation.[12] Ago proteins initially bind their target through base pairing with the seed segment of the guide (nucleotides 2−7 for human Ago).[13−15] Crystal structures have revealed that Ago preorders this seed segment into a helical conformation, allowing for the formation of a double helix between guide and target, and hence effectively prepaying the entropic cost of target binding.[16,17] This results in binding rates that are near diffusion limited (~10^7 M^{-1} s^{-1}).[18−21] In prokaryotes, there is a broad diversity of Agos with respect to the identity of their guide (RNA/DNA) and their target (RNA/DNA).[22,23] Some well-characterized prokaryotic Ago nucleases (*Tt*Ago, *Cb*Ago) use DNA guides to target single-stranded (ss)DNA.[24,25]

Here we describe a new DNA-PAINT method based on protein-assisted delivery of DNA imager strands, which allows for faster acquisition of super-resolved nanostructures. We use a wild-type Ago protein from the bacterium *Clostridium butyricum* (*Cb*Ago) to speed up the kinetic binding of DNA imager strands. *Cb*Ago reshapes the binding landscape of the imager strand, resulting in a 10-fold higher binding rate compared to conventional DNA-PAINT. Ago-PAINT can be implemented without additional complexity while retaining the programmability and specificity of DNA-PAINT, due to the favorable targeting feature of *Cb*Ago.[25,26] We determine the spatial resolution of Ago-PAINT through the use of 2D DNA origami structures and show that Ago-PAINT generates super-

https://dx.doi.org/10.1021/acs.nanolett.9b04277
Nano Lett. 2020, 20, 2264−2270

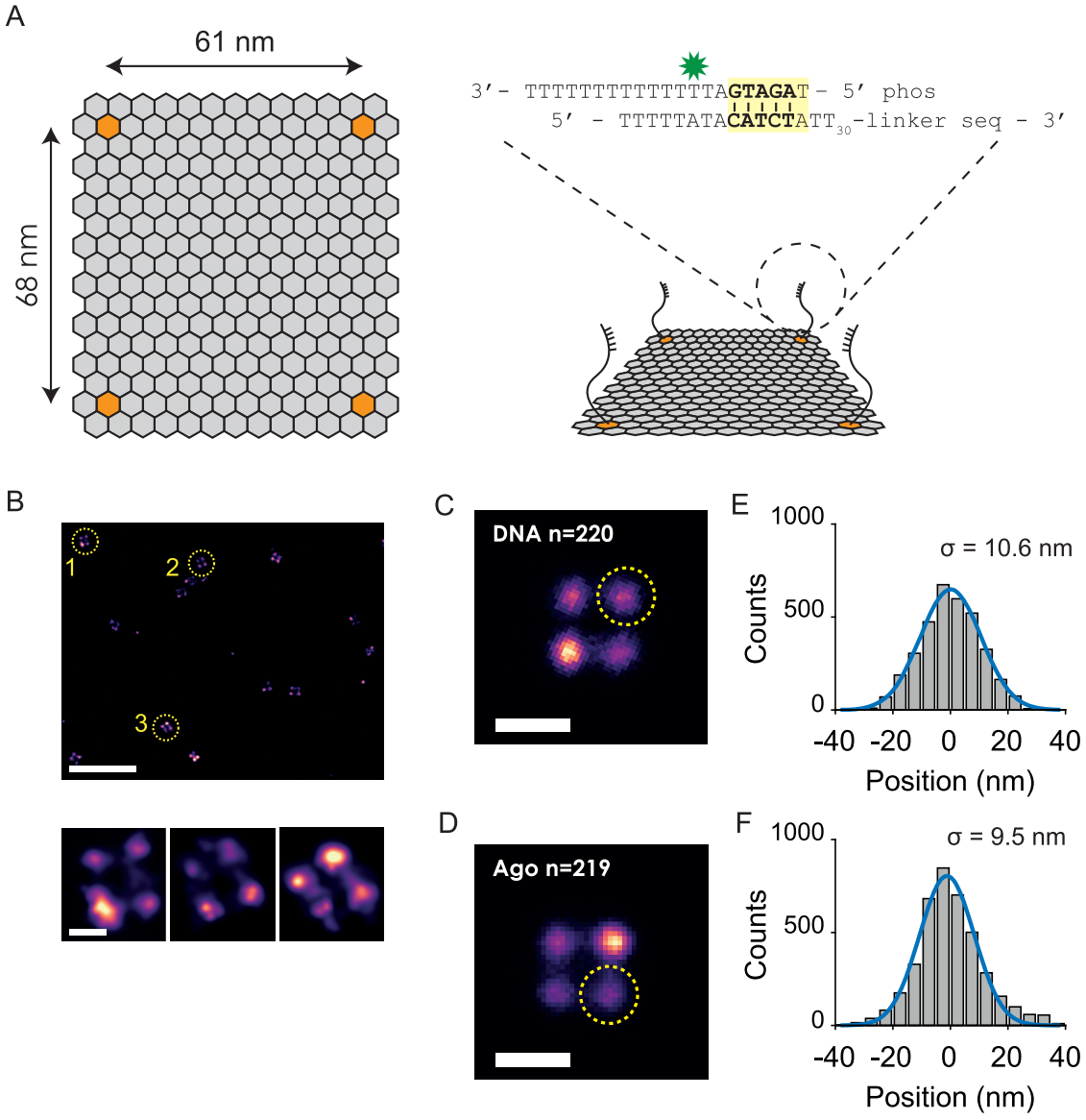

Figure 2. Ago-PAINT enables the same localization precision as conventional DNA-PAINT. (A) Left: A schematic design of the 2D-DNA origami structure. The orange honeycombs indicate the approximate locations of binding sites. Right: 3D representation of the imaging scheme with the docking strand sequence. The green star indicates the position of the Cy3 dye labeled on aminomodified thymine. (B) A representative super-resolution image showcasing binding sites of the 2D-DNA origami structures using Ago-PAINT. Bottom: Super-resolution reconstruction of the four-corner origami structures of the top panel. (C) A summed image of 220 origami structures visualized through the use of DNA-PAINT. (D) A summed image of 219 origami structures made through the use of Ago-PAINT. The concentration of the imager strand was 1 nM for both DNA-PAINT and Ago-PAINT. (E) Fitting of a cross-sectional intensity histogram from the yellow encircled area in panel C to a Gaussian (blue line) shows a localization precision of 10.6 nm. (F) Fitting of a cross-sectional intensity histogram from the yellow encircled area in panel D to a Gaussian (blue line) showing a localization precision of 9.5 nm. Scale bars in panel B indicate 500 nm (top) and 50 nm (bottom three). Scale bars in panels C and D indicate 100 nm.

resolution images of diffraction-limited structures at least 10-fold faster than conventional DNA-PAINT.

Results. For high-quality super-resolution images, a PAINT-based method requires more than five transient binding events per localization spot, each with a dwell time of at least several hundreds of milliseconds.[7−9] A typical 8-nt DNA-PAINT imager strand exhibits an on-rate of ∼10^6 M^{-1} s^{-1} and a dwell time (=1/off-rate) of ∼1 s.[9] DNA-PAINT experiments use an imager strand concentration between 1 and 10 nM. This range is chosen to be high enough to obtain a sufficient number of binding events during the acquisition time, but not too high to avoid cross-talk localization between structures.[7]

We determined the on- and off-rates of Ago-PAINT imager strands and compared these to the on- and off-rates of conventional DNA-PAINT with the same imager strands using a smFRET assay (Figure 1). Acceptor (Cy5)-labeled ssDNA targets were immobilized through biotin−streptavidin conjugation on a PEGylated quartz slide. Next, either donor (Cy3)-labeled 8-nt DNA-PAINT imager strands or Ago-PAINT imager strands (*Cb*Ago loaded with a Cy3-labeled guide) were injected, and their interactions with the immobilized target strand were probed using TIRF microscopy

https://dx.doi.org/10.1021/acs.nanolett.9b04277
Nano Lett. 2020, 20, 2264−2270

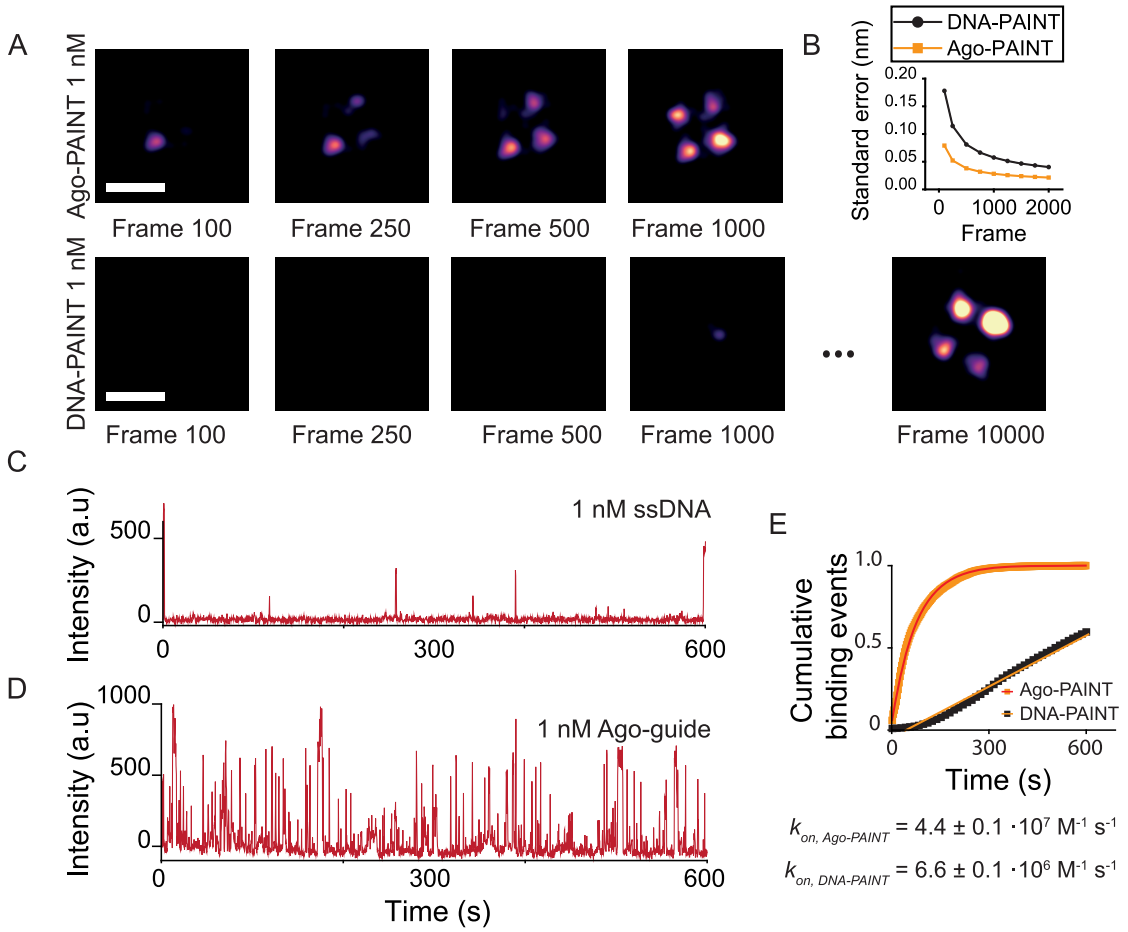

Figure 3. Ago-PAINT enables fast imaging of super-resolved structures. (A) Snapshots in time for Ago-PAINT (top) and DNA-PAINT (bottom) showing super-resolution images being formed over time. Exposure time: 0.3 s. The same color scale is used for the intensity in all images. (B) Standard error of Ago-PAINT vs DNA-PAINT plotted versus frame number. (C) Representative intensity vs time data trace of DNA-PAINT at 1 nM DNA concentration showing few binding events occurring within 600 s. The raw data trace is taken from a single origami plate. (D) Representative intensity vs the time data trace of the 1 nM Ago-guide complex showing binding events that occur frequently within 600 s. The raw data trace is taken from a single origami plate. (E) Normalized cumulative distribution of dark times (the time between binding events) for DNA-PAINT (black, n = 4870) and Ago-PAINT (orange, n = 5793). A single-exponential growth curve is used to estimate the binding rate for DNA-PAINT (orange) and a linear fit is used for a first order approximation for DNA-PAINT (red). Scale bars in panel A indicate 100 nm.

(Figure 1A). The assay was designed to give a high FRET signal upon specific binding of either DNA imager strand or Ago-guide complex to the complementary target (Figure 1B,C). The Cy3 position was picked the same as in previous studies with *Cb*Ago, to prevent any photophysical artifacts from occurring.[26,27] The time between the introduction of the imager strands and the first binding event is the apparent arrival time (which is the inverse of the on-rate, k_{on}). The duration of the FRET binding events is the dwell time (Figure 1B).

For a comparison between Ago-PAINT and DNA-PAINT, we designed an 8-nt DNA-PAINT imager strand (Figure 1C) and found that, under our experimental conditions, the average dwell time of this imager strand is 1.1 ± 0.2 s (Figure 1D). Next, we sought to find an Ago-PAINT guide with a similar dwell time. The first nucleotide of an Ago guide is embedded within the protein structure (Figure S1A).[16,17] Therefore, we determined the dwell time of Ago-guide complexes with different numbers (N) of base pairing with the target starting from the second nucleotide onward (Figure S1B). A guide with N = 5 (nt 2−6) base pairing to the target exhibited a comparable dwell time of 1.2 ± 0.2 s (Figure 1E). We observed that, for Ago-PAINT, the apparent arrival time is influenced by the number of base pairs that are formed between the guide and its target. For N = 5 or larger, the on-rate reaches a saturated value (k_{on} = 8.3 ± 0.8 × 10^{7} M^{-1} s^{-1}) (Figures 1F and S1C). Those values are 10 times higher than the typical on-rates for an 8-nt DNA-PAINT imager strand, 8.7 ± 0.8 × 10^{6} M^{-1} s^{-1} (Figure 1F).

To demonstrate the use of Ago-PAINT for super-resolution imaging, we designed a rectangular two-dimensional DNA origami structure of 76 nm × 80 nm (Figure 2 and Figure S2). The DNA origami structure has four docking sites that are spaced 61 nm × 68 nm apart (Figure 2A). To achieve optimal Ago binding to the DNA origami docking strands, we introduced a polyT linker between the target sequence of Ago and the DNA origami structure (Figure 2A, right panel). As our previous observation with *Cb*Ago[26] suggested that the protein occupies a footprint of around 20 nt, we made the length of polyT to be 30 nt.

Next, we sought to compare the localization precision of Ago-PAINT and DNA-PAINT. We tested our Ago-PAINT approach by injecting guide-loaded Ago into our flow cell in which DNA origami structures were immobilized. A super-

https://dx.doi.org/10.1021/acs.nanolett.9b04277
Nano Lett. 2020, 20, 2264−2270

resolution image could be reconstructed from the Ago-PAINT data, which revealed four detectable spots on the origami structures as expected from our assay design (Figure 2B). We determined the localization precision by selecting 220 origami structures for DNA-PAINT and 219 structures for Ago-PAINT and created a sum image using the Picasso analysis software[7] (Figure 2C,D). The localization precision was determined by plotting the cross-sectional histogram of one of the four binding sites of the summed DNA origami structure. For DNA-PAINT, this resulted in a localization precision of 10.6 nm (Figure 2E), and for Ago-PAINT, we found a localization precision of 9.5 nm (Figure 2F). The histogram demonstrates that Ago-PAINT delivers the same quality of localization precision when compared to the DNA-PAINT approach. Nearest neighbor analysis[28] reconfirms that the localization precision is similar for both Ago-PAINT and DNA-PAINT (Figure S3). Additionally, we probed the possibility of using different linker lengths for Ago-PAINT imaging. When we tested DNA origami structures with longer linkers (50 thymines or 100 thymine nucleotides), we found that this did not affect the localization precision of Ago-PAINT (Figures S4 and S5), showing that Ago-PAINT is compatible with various linker lengths (≥T30).

Finally, we compared the speed of super-resolution imaging through Ago-PAINT with the conventional DNA-PAINT approach using the 2D DNA origami structures as a testing platform. We evaluated the quality of a super-resolution image after each time point for both Ago-PAINT and DNA-PAINT (Figure 3A). The overall resolution of a single-molecule localization microscopy image is dependent on the number of localizations per docking strand. Therefore, to quantify the speed of imaging, we plotted the standard error of the localization precision as a function of frame number (Figure 3B), where we took the sigma values from Figure 2E,F as the localization precision. We observed that the standard error of the localization precision for Ago-PAINT is smaller than that of DNA-PAINT at each time point, indicating that super-resolved images of identical resolution will be obtained 10× faster through Ago-PAINT compared to DNA-PAINT. This result is further supported by the intensity vs time traces, which shows that our Ago-PAINT method results in more binding events compared to the DNA-PAINT approach, under similar conditions with DNA concentrations of 1 nM (Figure 3C−E and Figure S6). The on-rates for both Ago-PAINT (k_{on} = 4.4 ± 0.1 × 10^7 M^{-1} s^{-1}) and DNA-PAINT (k_{on} = 6.6 ± 0.1 × 10^6 M^{-1} s^{-1}) on our DNA-origami structure (Figure 3E) are similar to the on-rates that we found in our single-molecule experiments (Figure 1F).

Discussion. Here we presented a proof-of-concept of Ago-PAINT that allows for rapid super-resolution imaging. We demonstrated that fast Ago-PAINT recording can be used to acquire super-resolution images of nanostructures while retaining the programmability and predictability of DNA-PAINT.

For the visualization of several complex cellular components in a single cell, multiplexing super-resolution is highly anticipated. Recent developments allow for temporal[29] and spectral[30] multiplexing of DNA-PAINT and we believe that these methods can be integrated with Ago-PAINT. Also, in our previous work, we showed that different guide sequences resulted in distinctly different binding kinetics.[25] This kinetic fingerprinting will allow for additional freedom when designing multiplexing Ago-PADelfINT.[29,31] Furthermore, optimization of the imager sequence and imaging conditions allowed for a further increase in acquisition time for DNA-PAINT.[32] Although the binding kinetics or Ago-PAINT are near diffusion limited, we expect that optimization of the guide sequence could further improve the kinetics Ago-PAINT.

In this study, Ago-PAINT experiments are performed with the wild-type *Cb*Ago protein, which substantially increases the probe size compared to conventional DNA-PAINT. However, successful applications of Argonaute proteins for *in vivo* gene silencing[33,34] hint that our Ago-PAINT approach could be used in cellular super-resolution imaging. While targeting complex cellular structures in cells could be an issue with full-size *Cb*Ago, it is possible to use truncated versions of Ago. Some truncated versions of approximately half the size (short Agos) exist in nature.[22] We speculate that it will be possible to truncate them further as Ago-PAINT only relies on the property of preforming the helix structure of the imager strand. For example, an Ago variant from *Kluyveromyces polysporus* that contains only the C-lobe was reported to retain almost all of the binding properties of the untruncated version.[35] Furthermore, as the imager strand is loaded and protected inside the protein, degradation of the imager strand is less likely to occur over time, unlike oligos that are rapidly digested.[36]

In this Letter, we demonstrated the use of *Cb*Ago for super-resolution microscopy. While this *Cb*Ago targets ssDNA, Agos from other species can target RNA.[22] For example, the Ago from *Marinitoga piezophila* (*Mp*Ago)[37,38] targets RNA, and one could harness the property of a high association rate for other single-molecule imaging applications such as RNA sensing. Recently, *dTt*Ago has been combined with FISH[39] to allow for labeling of genomic loci in fixed cells. We anticipate the use of RNA-guided Agos for a significant speed-up in similar applications for RNA FISH. Lastly, complementary approaches such as DNA-based STED imaging,[40] qPAINT,[41] or cross-linking on a single-molecule target using Action-PAINT[42] could be combined with our Ago-PAINT approach. We envision the use of Ago-PAINT as a general toolkit to speed up many current existing applications that rely on base-pairing interactions.

■ ASSOCIATED CONTENT

Supporting Information

The Supporting Information is available free of charge at https://pubs.acs.org/doi/10.1021/acs.nanolett.9b04277.

Kinetics of different AgoPAINT probes, the DNA origami design and quality controls, AgoPAINT results for origami experiments with different linker lengths, and all materials and methods including DNA sequences used for DNA origami (PDF)

■ AUTHOR INFORMATION

Corresponding Author

Chirlmin Joo − *Department of BioNanoScience, Kavli Institute of Nanoscience, Delft University of Technology, 2629 HZ Delft, The Netherlands;* orcid.org/0000-0003-2803-0335; Email: c.joo@tudelft.nl

Authors

Mike Filius − *Department of BioNanoScience, Kavli Institute of Nanoscience, Delft University of Technology, 2629 HZ Delft, The Netherlands*

https://dx.doi.org/10.1021/acs.nanolett.9b04277
Nano Lett. 2020, 20, 2264−2270

Tao Ju Cui − *Department of BioNanoScience, Kavli Institute of Nanoscience, Delft University of Technology, 2629 HZ Delft, The Netherlands*
Adithya N. Ananth − *Department of BioNanoScience, Kavli Institute of Nanoscience, Delft University of Technology, 2629 HZ Delft, The Netherlands; Netherlands Organization for Applied Scientific Research (TNO), 2600 AD Delft, The Netherlands*
Margreet W. Docter − *Department of BioNanoScience, Kavli Institute of Nanoscience, Delft University of Technology, 2629 HZ Delft, The Netherlands*
Jorrit W. Hegge − *Laboratory of Microbiology, Wageningen University, 6703 HB Wageningen, The Netherlands*
John van der Oost − *Laboratory of Microbiology, Wageningen University, 6703 HB Wageningen, The Netherlands*

Complete contact information is available at: https://pubs.acs.org/10.1021/acs.nanolett.9b04277

Author Contributions

M.F. and T.J.C. contributed equally to this work. M.F., T.J.C., and C.J. conceived the project and designed the experiments. M.F., T.J.C., A.N.A, and C.J. designed and made the 2D DNA origami structure. J.W.H. and J.v.d.O. expressed and purified *Cb*Ago. M.F. and T.J.C. performed all single-molecule and DNA origami experiments. M.F., T.J.C., and M.W.D. analyzed the data. M.F., T.J.C. and C.J. wrote the manuscript. All authors read and improved the manuscript.

Notes

The authors declare no competing financial interest.

■ ACKNOWLEDGMENTS

We thank Carolien Bastiaanssen, Sung Hyun Kim, and Bernd Rieger for critical reading and feedback. C.J. was supported by Vidi (864.14.002) of The Netherlands Organization for Scientific Research; an ERC Consolidator Grant (819299) of the European Research Council; and Vrije Programma (SMPS) of the Foundation for Fundamental Research on Matter. A.N.A. acknowledges TNO for seed ERP-Bio Nano programme for funding.

■ REFERENCES

(1) Betzig, E.; et al. Imaging Intracellular Fluorescent Proteins at Nanometer Resolution. *Science (Washington, DC, U. S.)* **2006**, *313*, 1642−1645.
(2) Rust, M. J.; Bates, M.; Zhuang, X. Sub-diffraction-limit imaging by stochastic optical reconstruction microscopy (STORM). *Nat. Methods* **2006**, *3*, 793−796.
(3) Giannone, G.; et al. Dynamic Superresolution Imaging of Endogenous Proteins on Living Cells at Ultra-High Density. *Biophys. J.* **2010**, *99*, 1303−1310.
(4) Schoen, I.; Ries, J.; Klotzsch, E.; Ewers, H.; Vogel, V. Binding-activated localization microscopy of DNA l. *Nano Lett.* **2011**, *11*, 4008−4011.
(5) Sharonov, A.; Hochstrasser, R. M. Wide-field subdiffraction imaging by accumulated binding of diffusing probes. *Proc. Natl. Acad. Sci. U. S. A.* **2006**, *103*, 18911−18916.
(6) Jungmann, R.; et al. Multiplexed 3D cellular super-resolution imaging with DNA-PAINT and Exchange-PAINT. *Nat. Methods* **2014**, *11*, 313−318.
(7) Schnitzbauer, J.; Strauss, M. T.; Schlichthaerle, T.; Schueder, F.; Jungmann, R. Super-resolution microscopy with DNA-PAINT. *Nat. Protoc.* **2017**, *12*, 1198−1228.
(8) Dai, M.; Jungmann, R.; Yin, P. Optical imaging of individual biomolecules in densely packed clusters. *Nat. Nanotechnol.* **2016**, *11*, 798−807.
(9) Jungmann, R.; et al. Single-Molecule Kinetics and Super-Resolution Microscopy by Fluorescence Imaging of Transient Binding on DNA Origami. *Nano Lett.* **2010**, *10*, 4756−4761.
(10) Auer, A.; Strauss, M. T.; Schlichthaerle, T.; Jungmann, R. Fast, Background-Free DNA-PAINT Imaging Using FRET-Based Probes. *Nano Lett.* **2017**, *17*, 6428−6434.
(11) Lee, J.; Park, S.; Kang, W.; Hohng, S. Accelerated super-resolution imaging with FRET-PAINT. *Mol. Brain* **2017**, *10*, 63.
(12) Bartel, D. P. MicroRNAs: Target Recognition and Regulatory Functions. *Cell* **2009**, *136*, 215−233.
(13) Baek, D.; et al. The impact of microRNAs on protein output. *Nature* **2008**, *455*, 64−71.
(14) Selbach, M.; et al. Widespread changes in protein synthesis induced by microRNAs. *Nature* **2008**, *455*, 58.
(15) Guo, H.; Ingolia, N. T.; Weissman, J. S.; Bartel, D. P. Mammalian microRNAs predominantly act to decrease target mRNA levels. *Nature* **2010**, *466*, 835−840.
(16) Wang, Y.; et al. Structure of an argonaute silencing complex with a seed-containing guide DNA and target RNA duplex. *Nature* **2008**, *456*, 921−926.
(17) Schirle, N. T.; MacRae, I. J. The Crystal Structure of Human Argonaute2. *Science (Washington, DC, U. S.)* **2012**, *336*, 1037−1040.
(18) Chandradoss, S. D.; Schirle, N. T.; Szczepaniak, M.; Macrae, I. J.; Joo, C. A Dynamic Search Process Underlies MicroRNA Targeting. *Cell* **2015**, *162*, 96−107.
(19) Salomon, W. E.; et al. Single-Molecule Imaging Reveals that Argonaute Reshapes the Binding Properties of Its Nucleic Acid Guides. *Cell* **2015**, *162*, 84−95.
(20) Jo, M. H.; et al. Human Argonaute 2 Has Diverse Reaction Pathways on Target RNAs. *Mol. Cell* **2015**, *59*, 117−124.
(21) Yao, C.; Sasaki, H. M.; Ueda, T.; Tomari, Y.; Tadakuma, H. Single-Molecule Analysis of the Target Cleavage Reaction by the Drosophila RNAi Enzyme Complex. *Mol. Cell* **2015**, *59*, 125−132.
(22) Swarts, D. C.; et al. The evolutionary journey of Argonaute proteins. *Nat. Struct. Mol. Biol.* **2014**, *21*, 743−53.
(23) Hegge, J. W.; Swarts, D. C.; Van Der Oost, J. Prokaryotic argonaute proteins: Novel genome-editing tools? *Nat. Rev. Microbiol.* **2018**, *16*, 5−11.
(24) Swarts, D. C.; et al. DNA-guided DNA interference by a prokaryotic Argonaute. *Nature* **2014**, *507*, 258−61.
(25) Hegge, J. W.; et al. DNA-guided DNA cleavage at moderate temperatures by Clostridium butyricum Argonaute. *Nucleic Acids Res.* **2019**, *47*, 5809−5821.
(26) Cui, T. J.; Klein, M.; Hegge, J. W.; Chandradoss, S. D.; van der Oost, J.; Depken, M.; Joo, C.; et al. Argonaute bypasses cellular obstacles without hindrance during target search. *Nat. Commun.* **2019**, *10*, 4390.
(27) Hegge, J. W.; et al. DNA-guided DNA cleavage at moderate temperatures by Clostridium butyricum Argonaute. *Nucleic Acids Res.* **2019**, *47*, 5809−5821.
(28) Endesfelder, U.; Malkusch, S.; Fricke, F.; Heilemann, M. A simple method to estimate the average localization precision of a single-molecule localization microscopy experiment. *Histochem. Cell Biol.* **2014**, *141*, 629−638.
(29) Wade, O. K.; et al. 124-Color Super-resolution Imaging by Engineering DNA-PAINT Blinking Kinetics. *Nano Lett.* **2019**, *19*, 2641−2646.
(30) Deußner-Helfmann, N. S.; et al. Correlative Single-Molecule FRET and DNA-PAINT Imaging. *Nano Lett.* **2018**, *18*, 4626−4630.
(31) Shah, S.; Dubey, A. K.; Reif, J. Programming Temporal DNA Barcodes for Single-Molecule Fingerprinting. *Nano Lett.* **2019**, *19*, 2668−2673.
(32) Schueder, F.; et al. An order of magnitude faster DNA-PAINT imaging by optimized sequence design and buffer conditions. *Nat. Methods* **2019**, *16*, 1101−1104.

(33) Wittrup, A.; Lieberman, J. Knocking down disease: a progress report on siRNA therapeutics. *Nat. Rev. Genet.* **2015**, *16*, 543−552.
(34) Setten, R. L.; Rossi, J. J.; Han, S. The current state and future directions of RNAi-based therapeutics. *Nat. Rev. Drug Discovery* **2019**, *18*, 421−446.
(35) Dayeh, D. M.; Cantara, W. A.; Kitzrow, J. P.; Musier-Forsyth, K.; Nakanishi, K. Argonaute-based programmable RNase as a tool for cleavage of highly-structured RNA. *Nucleic Acids Res.* **2018**, *46*, e98.
(36) Tyagi, S. Imaging intracellular RNA distribution and dynamics in living cells. *Nat. Methods* **2009**, *6*, 331−338.
(37) Kaya, E.; et al. A bacterial Argonaute with noncanonical guide RNA specificity. *Proc. Natl. Acad. Sci. U. S. A.* **2016**, *113*, 4057−4062.
(38) Lapinaite, A.; Doudna, J. A.; Cate, J. H. D. D. Programmable RNA recognition using a CRISPR-associated Argonaute. *Proc. Natl. Acad. Sci. U. S. A.* **2018**, *115*, 3368−3373.
(39) Chang, L.; et al. AgoFISH: cost-effective in situ labelling of genomic loci based on DNA-guided dTtAgo protein. *Nanoscale Horizons* **2019**, *4*, 918−923.
(40) Spahn, C.; et al. Protein-Specific, Multicolor and 3D STED Imaging in Cells with DNA-Labeled Antibodies. *Angew. Chem., Int. Ed.* **2019**, *58*, 18835−18838.
(41) Jungmann, R.; et al. Quantitative super-resolution imaging with qPAINT. *Nat. Methods* **2016**, *13*, 439−442.
(42) Liu, N.; Dai, M.; Saka, S. K.; Yin, P. Super-resolution labelling with Action-PAINT. *Nat. Chem.* **2019**, *11*, 1001−1008.

https://dx.doi.org/10.1021/acs.nanolett.9b04277
Nano Lett. 2020, 20, 2264−2270